A Copper(I)-Complexed Rotaxane with Two Fullerene Stoppers: Synthesis, Electrochemistry, and Photoinduced Processes.

Nicola Armaroli,* François Diederich,* Christiane O. Dietrich-Buchecker, Lucia Flamigni,* Giancarlo Marconi, Jean-François Nierengarten, and Jean-Pierre Sauvage*

Dedicated to Professor Vincenzo Balzani on the occasion of his 60th birthday

Abstract: A rotaxane made from a bisphenanthroline Cu^I complex and two C_{60} units acting as stoppers has been synthesized**.** Electrochemical, spectroscopic and photophysical properties of the individual components, a methanofullerene and a Cu^I catenate, were determined. The properties of the methanofullerene were also compared with those of plain C_{60} and rationalized with the aid of semiempirical calculations. The changes in the photophysical properties detected in the rotaxane with respect to the models were assigned to the occurrence of intramolecular processes. The excited singlet state localized on the fullerene and the MLCT excited state centred on the Cu^I complex are both quenched. Deactivation of the fullerene excited singlet state occurs by energy transfer to the Cu^I-complex moiety, which competes with intersystem crossing to triplet fullerene, whereas the Cu^I-complex excited state is mainly quenched by electron transfer to form the charge-separated state consisting of the oxidized metal centre $[Cu(phen)_2]^{2+}$ and the fullerene radical anion. The fullerene triplet, formed in reduced yield with respect to the model, is also quenched by electron transfer to the same charge-separated state. The ability of both model components to sensitize singlet oxygen is completely suppressed in the rotaxane. The occurrence of a fast back-electron-transfer reaction is postulated, as spectroscopic detection of the charge-separated state has not been achieved.

Keywords: copper • electrochemistry • electron transfer • fullerenes • rotaxanes

Introduction

Since the discovery of buckminsterfullerene (C_{60}),[1] an increasing number of scientists have devoted their attention to this new material, its derivatives,[2] and its higher homologues[3] as attested by the spectacular development of the literature in this field.[4] This new carbon allotrope has the unusual power of exciting the interest of researchers in many fields including theoretical, experimental and applied chemistry. Inter alia, C_{60} has been extensively characterized photo-[5] and electrochemically[6] showing remarkable properties such as: i) electronic absorption bands throughout the entire UV/Vis spectral region;[7] ii) strong and characteristic singlet–singlet[8] and triplet–triplet transient absorption features;[9] iii) a weak fluorescence at room temperature[10] and 77 K[11a–c] and a phosphorescence band only in a rigid matrix;[11c–e] iv) sensitization of singlet oxygen[12] with unitary efficiency;[13] and v) a strong-electron acceptor character, as indicated by the presence of four to six fully reversible reduction processes[14] depending on the solvent. Accordingly, many investigations have been carried out on ground-state charge-transfer complexes and photoinduced electron transfer between C_{60} and a variety of electron donors, including amines[15] and polymer substrates.[16] By contrast, to date little work has been reported on the photochemical and photophysical properties of supramolecular assemblies containing fullerene subunits,[17] although the above-mentioned properties show promise for the promotion of electron-transfer processes in suitably assembled supramolecular arrays. The study of such processes is of interest for many fundamental and practical purposes, which include a better understanding of natural photosynthesis[18] and the construction of photochemical molecular devices[19] capable of performing useful functions such as i) the conversion of solar light into fuel and

---

[*] Dr. J.-P. Sauvage, Dr. C.O. Dietrich-Buchecker
Laboratoire de Chimie Organo-Minérale, Université Louis Pasteur
Faculté de Chimie, 4, rue Blaise Pascal
F-67070 Strasbourg (France)
Fax: (+33) 3-88-607312
E-mail: sauvage@chimie.u-strasbg.fr

Dr. N. Armaroli, Dr. L. Flamigni, Dr. G. Marconi
Istituto di Fotochimica e Radiazioni d'Alta Energia del CNR
via Gobetti 101, I-40129 Bologna (Italy)
E-mail: armaroli@bofra3.frae.bo.cnr.it
E-mail: flamigni@bofra3.frae.bo.cnr.it

Prof. Dr. F. Diederich, Dr. J.-F. Nierengarten
Laboratorium für Organische Chemie, ETH-Zentrum
Universitätstrasse 16, CH-8092 Zürich (Switzerland)
E-mail: diederich@org.chem.ethz.ch

0947-6539/98/0403-0406 $ 17.50+.50/0

electricity,[20] ii) the chemical monitoring of the environment[21] and iii) the storage and elaboration of information at a molecular level.[22]

Given the good electron-accepting properties of C_{60}, a good electron-donor partner is required to favour photoinduced electron transfer in a supramolecular array. We thought that a Cu^I bisphenanthroline complex could be a good choice in this respect for many reasons, the first of which is that such complexes are known to be potent reductants in the excited state.[23] In addition, when the phenanthroline ligands are substituted in the 2,9 positions by aryl residues the complexes display excellent photostability, long-lived luminescent excited states and absorption spectra throughout the UV/Vis spectral region,[24] which make them potentially useful for harvesting solar-energy. Finally, it should be pointed out that the outstanding affinity of Cu^I towards phenanthroline-type ligands allows the high-yield preparation of complex supramolecular structures such as catenanes, rotaxanes, knots and helicates.[25]

We report here the synthesis, electrochemical behaviour and excited state properties in CH_2Cl_2 solution of the rotaxane Si-C_{60}-Cu formed from a bisphenanthroline Cu^I complex and two C_{60}-type units which act as stoppers[26] (Figure 1). This combination of molecular components makes Si-C_{60}-Cu a good candidate to undergo photoinduced electron transfer. The photophysical properties of the rotaxane are compared with those of two suitable molecular models: a C_{60} methanofullerene (Si – C_{60})[27] and a Cu^I catenate (Cu – cat)[28] (Figure 2). The choice of Si – C_{60} and Cu – cat as reference compounds instead of **1**[27] and **2** (Figure 1), the direct precursors to the rotaxane, relies on the fact that the latter have rather unstable, unprotected terminal alkyne functions. A comparison between the photophysical properties of Si – C_{60} and plain C_{60} is also reported.

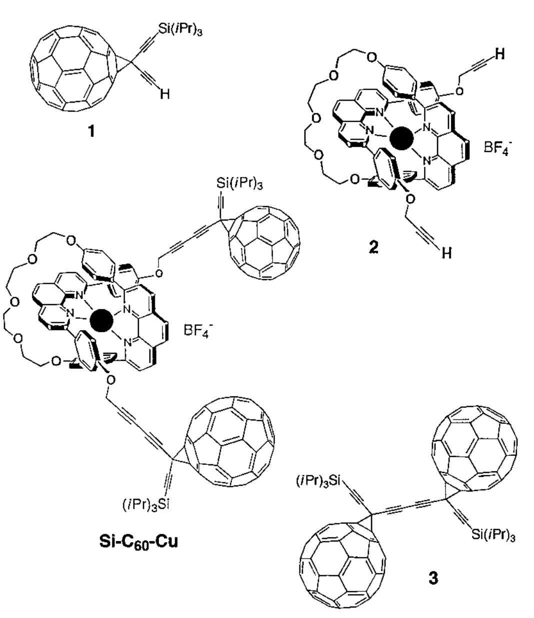

1 **2** **Si-C60-Cu** **3**

Figure 1. Schematic formulae of compounds **1**–**3** and Si-C_{60}-Cu (● = Cu^+).

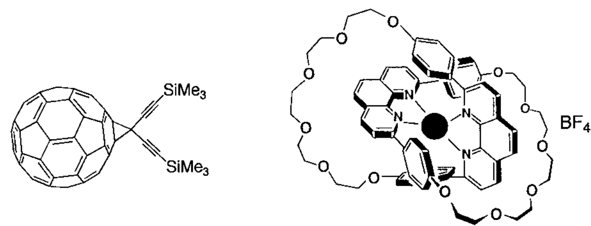

Si-C60 **Cu-cat**

Figure 2. Schematic formulae of Si – C_{60} and Cu – cat (● = Cu^+); the model compounds used in the photophysical investigations.

Results

Synthesis: An attractive and convenient route for the synthesis of the Cu^I-complexed rotaxane Si-C_{60}-Cu relies on the oxidative coupling reaction between the terminal alkynes **1** and **2**, which are accessible in gram quantities (Figure 1). It has been previously shown that acetylenic oxidative coupling reactions are compatible with both fullerene derivatives[27, 29] and bis(diphenylphenanthroline) Cu^I complexes.[30] Rotaxane Si-C_{60}-Cu was prepared by treating the multicomponent complex **2** with the methanofullerene derivative **1** under dry air in CH_2Cl_2 at room temperature in the presence of a large excess of Hay catalyst[31] [CuCl-*N,N,N′,N′*-tetramethylethylenediamine (TMEDA)]. When **1** and **2** were used in a 2.5:1 molar ratio, Si-C_{60}-Cu was only obtained in a low yield (3.5 %). The yield of Si-C_{60}-Cu could be improved to 15 % by the use of a 5:1 ratio of **1**:**2**. In addition to Si-C_{60}-Cu, the dimeric fullerene derivative **3**,[27] resulting from the homocoupling reaction of **1**, was also formed. Surprisingly, no [3]-catenane[30] formed as a result of the cyclodimerisation of the Cu^I complex **2** could be detected.

The Cu^I-complexed rotaxane Si-C_{60}-Cu with its two fullerene stoppers is reasonably soluble in CS_2, CH_2Cl_2 and $CHCl_3$. In the ^{13}C NMR spectrum ($CS_2/CDCl_3$, 1:1) a total of 49 out of the 51 expected resonances for the C_{2v}-symmetric compound Si-C_{60}-Cu (31 for the fullerene sp^2 carbons and 20 for the two diphenylphenanthroline fragments) are distinguishable in the aromatic and fullerene region and all 15 alkynyl and aliphatic signals are observed. The ^1H NMR spectrum is also in full accordance with the structure of Si-C_{60}-Cu. The FAB-MS (Figure 3) confirmed the structure of the Cu^I-complexed rotaxane with a very intense signal at $m/z = 2900.2$ corresponding to the pseudo-molecular-ion peak which results from the loss of the BF_4^- counteranion.

Electrochemistry: The redox properties of Si-C_{60}-Cu were studied by cyclic voltammetry in CH_2Cl_2 with 0.1M Bu_4NBF_4 as the electrolyte. Surprisingly, a significant anodic shift was observed for the reversible Cu-centred redox process in comparison with other similar mononuclear complexes.[32] For instance, the redox potential of the Cu(I/II) couple in Si-C_{60}-Cu appears at +0.865 V vs the saturated calomel electrode (SCE), whereas the potential of the Cu-localised redox process for the reference catenate (Cu – cat) is +0.565 V vs SCE in CH_3CN.[32] By contrast, in CH_2Cl_2 (vs SCE) the first reduction of both Si – C_{60} (– 0.520 V, rev) and the fullerene units of Si-C_{60}-Cu (– 0.6 V, irrev) appear in the range typical

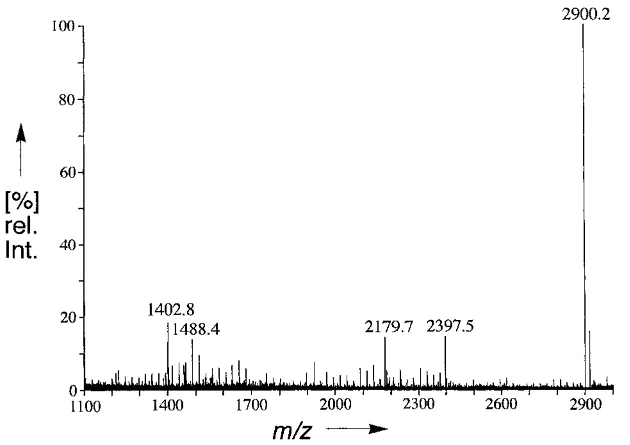

Figure 3. Positive ion FAB-mass spectrum of Si-C_{60}-Cu (in *m*-nitrobenzyl alcohol as the matrix) showing the pseudo-molecular-ion peak resulting from the loss of the BF_4^- counteranion at $m/z = 2900.2$ (calcd for $C_{210}H_{90}N_4O_7Si_2Cu$: 2900.8).

of C_{60} monoadducts.[6, 33] As previously observed for various bis(butadiynyl)methanofullerene derivatives,[34] Si-C_{60}-Cu undergoes reductive electrochemical polymerization during iterative cyclic voltammetry to give an insoluble, insulating film on the platinum cathode surface.

Steady-state absorption and luminescence properties: The electronic absorption spectra of Si-C_{60}-Cu, Si–C_{60} and Cu–cat in CH_2Cl_2 are depicted in Figure 4. In the UV region, the model fullerene compound Si–C_{60} displays two very intense bands ($\varepsilon_{max} = 10^4 - 10^5$ $M^{-1}cm^{-1}$) typical of fullerene derivatives. In the visible region, the spectrum is broad and much less intense ($\varepsilon_{max} = 10^3 - 10^2$ $M^{-1}cm^{-1}$), Table 1. An analogous pattern in the absorption intensities is displayed by Cu–cat. The molar extinction coefficients of Si-C_{60}-Cu cannot be evaluated because of solubility problems (see Experimental Section). Although the spectrum of Si-C_{60}-Cu displays some of the characteristic absorptions of both components, such as the typical weak fullerene monoadduct bands at 430 (sh) and 683 (sh) nm as well as the strong UV bands at 252 and 322 nm, the profile of the absorption spectrum of the rotaxane cannot be fully superimposed on the sum of the absorption spectra of the model compounds.

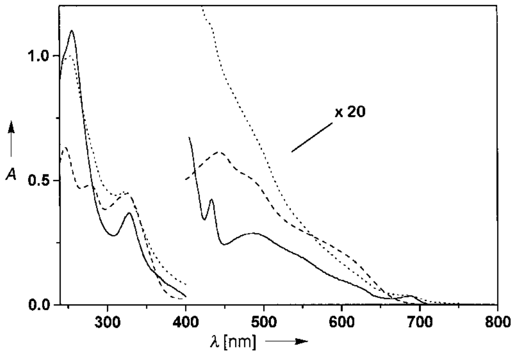

Figure 4. Electronic absorption spectra of Si–C_{60} (—), Cu–cat (- - -) and Si-C_{60}-Cu (···) in CH_2Cl_2. The concentration is 1.0×10^{-5} for Si–C_{60} and Cu–cat and is unknown for Si-C_{60}-Cu as a result of its low solubility (see text). In the 400–800 nm region the spectra are multiplied by a factor of 20.

The room-temperature emission spectra of isoabsorbing solutions (same absorbance at the excitation wavelength $\lambda_{exc} = 532$ nm) of Si-C_{60}-Cu, Si–C_{60} and Cu–cat are displayed in Figure 5.

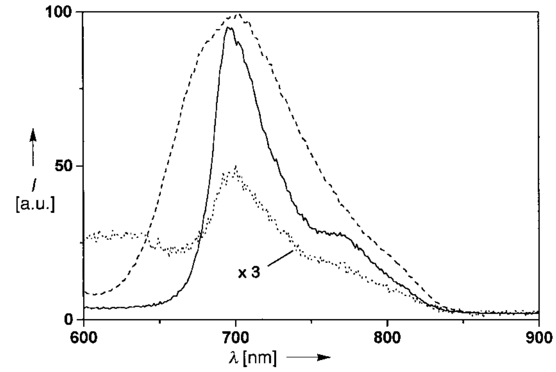

Figure 5. Luminescence spectra of isoabsorbing solutions of Si–C_{60} (—), Cu–cat (- - -) and Si-C_{60}-Cu (···) in CH_2Cl_2 at 293 K. At the excitation wavelength $\lambda_{exc} = 532$ nm, the light repartition in the supramolecular species Si-C_{60}-Cu is as follows: 40% on the central Cu^I complex,and 60% on the fullerene stoppers.

Incidentally, the emission maxima of Si–C_{60} and Cu–cat are almost coincident. For Si-C_{60}-Cu only a very weak emission was detected, whose shape is reminiscent of that of Si–C_{60} and C_{60}. In a rigid matrix of CH_2Cl_2 at 77 K, Si–C_{60} displays a fluorescence band ($\lambda_{max} = 715$ nm), while Cu–cat shows a very weak luminescence with $\lambda_{max} = 750$ nm. A very weak emission band ($\lambda_{max} = 715$ nm) was also observed for Si-C_{60}-Cu under the same experimental conditions. Any attempts to detect phosphorescence for Si–C_{60} (and also for plain C_{60}) were unsuccessful, even working with a time window that excludes the immediate fluorescence and also with a red-enhanced photomultiplier tube. Phosphorescence was also not observed in a transparent BuCN glass. Similar results were obtained by other authors.[11a–b, 35] Nonetheless, phosphores-

Table 1. Electronic absorption and luminescence data in CH_2Cl_2.

	Absorption, 293 K	Luminescence, 293 K			77 K
	λ_{max} ($\varepsilon \times 10^{-3}$) [nm ($M^{-1}cm^{-1}$)]	λ_{max}[a] (nm)	τ (ns)	$\Phi_{em} \times 10^4$	λ_{max} (nm)
C_{60}	257 (170); 329 (49); 404 (2.5); 538 (0.7); 594 (0.6)	723	1.3	1	700
Si–C_{60}	245 (sh, 99); 256 (110); 328 (37); 434 (2.1); 488 (1.4); 687 (0.2)	696	1.6	5	714
Cu–cat	247 (63); 278 (48); 325 (45); 440 (3.0)	703	175[b]	9	750
Si-C_{60}-Cu[c]	245 (sh); 252; 322; 430 (sh); 490 (sh); 683 (sh)	696	0.5; 1.7	0.8	710[d]

[a] From uncorrected emission spectra. [b] Deaerated solution, 125 ns in an air-equilibrated sample. [c] The molar extinction coefficients ε could not be evaluated as a result of the poor solubility of the sample (see text). [d] Extremely weak signal.

0947-6539/98/0403-0408 $ 17.50+.50/0

cence spectra attributed to C_{60} can be found in the literature in matrices below 5 K[11c, 11e] or at 77 K in the presence of heavy-atom-containing solvents.[11b]

The absorption and emission spectra of C_{60} are shown in Figure 6. A comparison of the absorption and emission properties of Si–C_{60} with plain C_{60} revealed that, in the UV region, the absorption bands of Si–C_{60} are less intense and less well resolved than for C_{60}. In the visible region the two compounds display rather different spectral features, which lead to the very distinct colours of the two species: Si–C_{60} is deep red, whereas C_{60} is magenta purple. It is worth noting that the spectrum of Si–C_{60} extends further into the red than that of C_{60}, showing the characteristic maximum of fullerene monoadducts at 687 nm.[36] Both species are luminescent; the emission bands have similar spectral positions, but a different pattern and C_{60} displays a higher energy onset. Si–C_{60} is a stronger luminophore than C_{60}, its emission quantum yield being 5 times higher at room temperature than that of C_{60} (Table 1). In a CH_2Cl_2 nontransparent matrix at 77 K, the fluorescence maxima of C_{60} and Si–C_{60} are located at 700 and 714 nm, respectively (Table 1), the latter being red-shifted with respect to room temperature (696 nm). The room-temperature excitation spectra of C_{60}, Si–C_{60} and Cu–cat, based on their emission maxima (Table 1), match the corresponding absorption profiles throughout the UV/Vis spectral region.

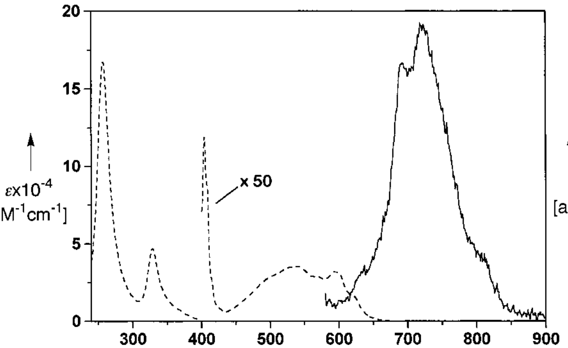

Figure 6. Absorption (- - -) and emission (—) spectra of C_{60} in CH_2Cl_2 solution at 293 K.

Time-resolved absorption and luminescence spectroscopy: It should be noted that at both excitation wavelengths used (355 and 532 nm) the partition of the photons among the chromophores of Si-C_{60}-Cu is 3:2 (Si–C_{60}:Cu–cat), calculated on the basis of the absorption coefficients of the two model compounds.

The streak images of the luminescence of C_{60} and Si–C_{60} show bands with maxima around 720 and 700 nm, respectively, which is in agreement with the steady-state luminescence. The luminescence lifetimes, measured on the time profiles taken around the maxima, are 1.3 ns for C_{60} and 1.6 ns for Si–C_{60}. The same experiment on Si-C_{60}-Cu shows an image with an emission band centred at 700 nm whose time profile fits well with biexponential kinetics, with lifetimes of 0.5 and 1.7 ns (Figure 7, Table 1) and a relative weight of 0.6 and 0.4, respectively.

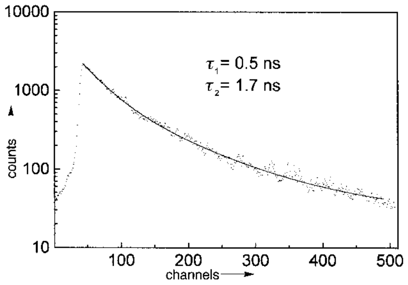

Figure 7. Time profile of the luminescence decay of the rotaxane Si-C_{60}-Cu in the 690–710 nm region. Solvent, CH_2Cl_2; $\lambda_{exc} = 532$ nm ($A = 0.2$); 3 mJ per pulse; 15.4 ps per channel. The data points have been fitted to a biexponential decay.

The picosecond time resolved absorption spectrum of the model Si–C_{60} displays both singlet–singlet ($\lambda_{max} = 520$ and 900 nm) and triplet–triplet ($\lambda_{max} = 700$ nm) features. The decay of the singlet bands matches the formation of the triplet, and isosbestic points are found at 570 and 750 nm. The lifetimes of singlet decay and triplet formation for Si–C_{60} coincide (1.5 ns) and are in good agreement with the singlet lifetime determined by the luminescence decay (1.6 ns, see above). In Figure 8, the time-resolved absorption spectra of C_{60} and Si–C_{60} are compared; the singlet and triplet absorption maxima of Si–C_{60} are at higher energy than those of C_{60}. This behaviour has already been observed for other monoadducts of C_{60}.[17a]

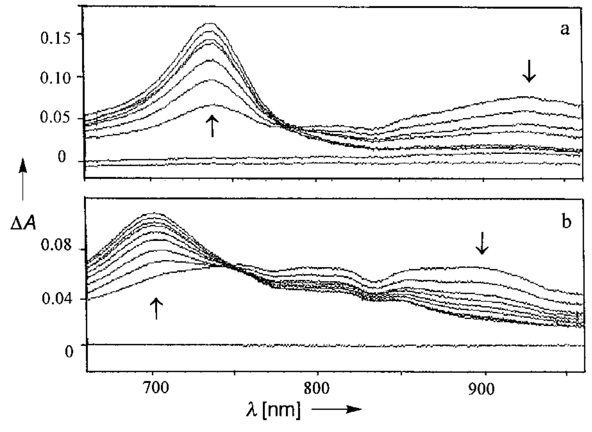

Figure 8. Transient absorption in the near infrared spectral region of a) C_{60} and b) Si–C_{60}. Solvent, CH_2Cl_2; $\lambda_{exc} = 532$ nm ($A = 0.14$); 4 mJ per pulse; time intervals 330 ps.

The picosecond transient absorption spectrum of Si-C_{60}-Cu, immediately after the laser pulse, displayed bands with maxima at 520 nm and 900 nm, which was also observed for Si–C_{60}. Nevertheless, the singlet band in the 400–600 nm region appeared wider and red-shifted in comparison with Si–C_{60} (Figure 9) because of the contribution of the Cu^I-complexed moiety, which is known to display a broad absorption band with a maximum at 585 nm.[37] The isosbestic points between singlet and triplet in Si-C_{60}-Cu are no longer present, an indication that processes other than simple

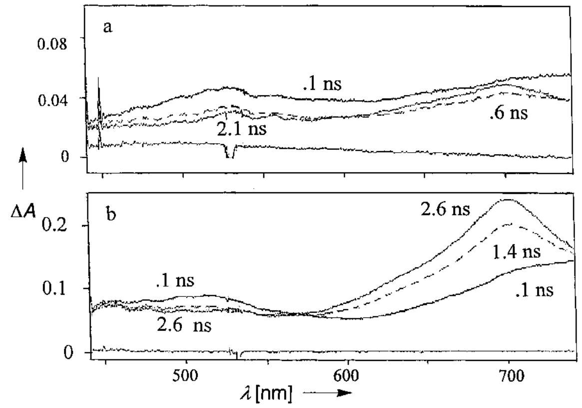

Figure 9. Transient absorption spectra in the visible spectral region of a) Si-C_{60}-Cu and b) Si–C_{60}. Solvent, CH_2Cl_2; $\lambda_{exc} = 532$ nm ($A = 0.14$); 7 mJ per pulse. The time values correspond to the delay at which the spectra are recorded after the 35 ps laser pulse.

intersystem crossing occur. Figure 10 shows the time evolution of the triplet (700 nm) and the singlet (880 nm) excited-state absorbances in Si-C_{60}-Cu. It is evident that the singlet decay rate does not match the triplet formation, which appears to grow, at least in part, with a slower rate. The singlet band decays with a lifetime (0.4 ns) in good agreement with the shortest lifetime (0.5 ns) measured from the decay of the luminescence. The triplet appears to be formed with a rate constant ($\tau = 1.8$ ns) in agreement with the second, slower luminescence decay ($\tau = 1.7$ ns, see above).

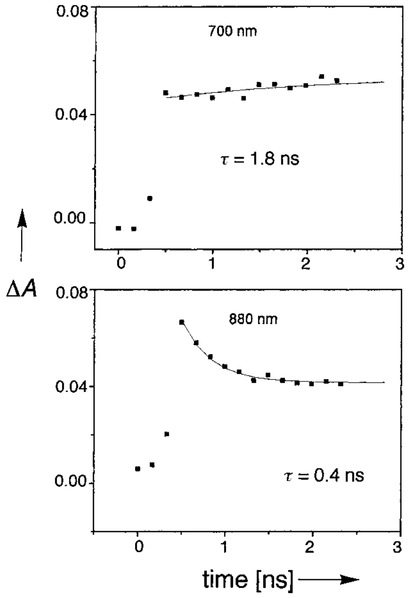

Figure 10. Differential absorption decay of a solution of Si-C_{60}-Cu in CH_2Cl_2, $\lambda_{exc} =$ 532 nm ($A = 0.14$), 7 mJ per pulse. The absorbances at 700 and 880 nm are attributed to the fullerene triplet and singlet, respectively.

The fully evolved triplet spectra of Si-C_{60}-Cu and the model compounds can be detected on a longer timescale with a nanosecond flash-photolysis apparatus. In Figure 11, the spectra of the triplets of Si–C_{60} and Si-C_{60}-Cu (oxygen-free, isoabsorbing solutions) are shown, together with that of C_{60} determined under the same experimental conditions.

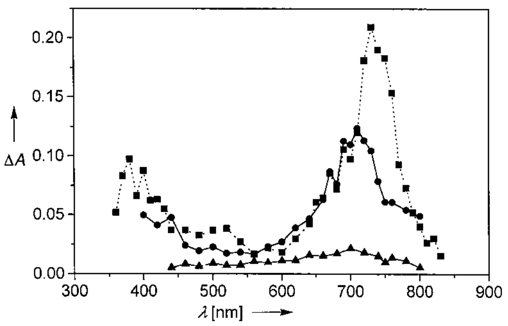

Figure 11. Transient absorption spectra recorded immediately after excitation with a 20 ns laser pulse; (■) C_{60}, (●) Si–C_{60}, (▲) Si-C_{60}-Cu. Solvent, CH_2Cl_2; $\lambda_{exc} = 355$ nm ($A = 1.1$); 1 mJ per pulse.

A quantitative estimate of the relative yield of Si-C_{60}-Cu triplet formation with respect to the model Si–C_{60} can be attempted by assuming the same absorption coefficients and by taking into account only the absorption of the fullerene moiety of the rotaxane (60% of the total incident light). As a result, the triplet formation in Si-C_{60}-Cu turns out to be about 30% that of the model Si–C_{60}. In Si–C_{60}, the decay of the triplet in deoxygenated solution is monoexponential with a lifetime of 5 μs, while in Si-C_{60}-Cu (where the yield of triplet formation is strongly decreased, see above) the triplet decay lifetime is 170 ns. The triplet absorption properties are summarized in Table 2. After the decay of the Si-C_{60}-Cu triplet, a residual minor component is observed with an absorbance of the order of $5-6 \times 10^{-3}$, a maximum around 740 nm and a lifetime of 1.7 μs in deoxygenated solutions.

Table 2. $T-T$ absorption properties[a] and $^1O_2$ sensitization[b] in CH_2Cl_2 solution at 293 K.

	λ_{max}(nm)	τ(μs)	$\varepsilon \times \Phi_{rel}$	$\Phi_{rel}(^1O_2)$
C_{60}	740	60	1	1
Si-C_{60}	700	5	0.6	0.82
Cu-cat	530, 585[c]	0.179[c]	–	0.11
Si-C_{60}-Cu	700	0.170	0.2[d]	0.03

[a] Oxygen-free solutions. [b] Air-equilibrated solutions. [c] From ref. [37]. [d] Calculated on the basis of the photon absorbed by the two fullerene moieties only (60% both at 532 and at 355 nm).

Under the same experimental conditions (1 mJ at 355 nm) C_{60} showed a nonexponential decay of the triplet; a drastic decrease in excitation energy down to a few μJ was necessary to obtain a reasonably exponential decay of 60 μs.

Experiments on sensitization of singlet-oxygen luminescence ($^1\Delta_g$)[12, 38] showed a dramatic decrease in the quantum yield of singlet-oxygen generation in passing from the two model compounds to the rotaxane. Taking pure C_{60} as a relative standard ($\Phi_{rel} = 1$), we measured values of 0.82, 0.11 and 0.03 for Si–C_{60}, Cu–cat and Si-C_{60}-Cu, respectively (Table 2).

Discussion

Model compounds Si–C_{60} and Cu–cat: The methanofullerene derivative Si–C_{60} displays absorption spectral features comparable with those of other monofunctionalized fullerenes,[2b–c, 36] attributable to slightly perturbed transitions of the parent compound C_{60}. In particular, in the visible region the typical 404 nm C_{60} band is absent and two new bands at 434 and 687 nm appear.

In order to gain insight into the nature of the excited states of this compound, a series of semiempirical calculations (Zerner intermediate neglect of differential overlap (ZINDO/1) hamiltonian[39] for geometry optimization and ZINDO for spectroscopy (ZINDO/S), with configuration interactions (CI) limited to 110 singly excited configurations, for spectroscopic transitions[40]) were carried out for both Si–C_{60} and C_{60}. The results of these calculations show that the lowest singlet excited state, calculated at 595 nm for the parent molecule, undergoes a large red shift (662 nm), which is in fairly good agreement with the appearance of the new band at 687 nm. In C_{60} the equivalent lowest excited state (T_{1g}) is forbidden by symmetry and is vibronically induced, whereas in Si–C_{60} the disruption of the high symmetry (I_h) makes it allowed with a calculated oscillator strength (f) of 0.012. This particular feature of Si–C_{60} is also reflected in its characteristic fluorescence properties, namely i) a red shift in the onset of the emission band (Figure 5), ii) a slightly longer singlet excited-state lifetime (Table 1) and iii) an increased emission quantum yield (Table 1).

The absorption spectrum of Si–C_{60} shows also that the lowest allowed singlet transition, which occurs at 404 nm for C_{60}, undergoes a red shift of ca. 30 nm and an intensity increase, two features consistently reproduced by the calculation ($\Delta\lambda = 41$ nm and $\Delta f = 0.03$). It has to be noted that an absorption band around 430 nm is characteristic of a wide class of monosubstituted fullerenes,[2b–c, 36] and that in optically active molecules the strong circular dichroism signal associated with this band has been used to determine the absolute configuration.[41]

As far as the lowest triplet manifold of Si–C_{60} is concerned, one observes a large decrease of the triplet lifetime (5 µs) compared with C_{60} (60 µs). This fact, which is also reflected in the better ability of C_{60} to sensitize singlet oxygen, could be rationalized on the basis of the heavy-atom effect on the intersystem-crossing process and/or a $T_1 - S_0$ energy gap more favourable for the silylated compound. Since the $S_1 \rightarrow T_1$ process, which should also be influenced by heavy atoms, appears quite unaffected upon substitution, the latter factor would appear to be responsible for enhancing the triplet deactivation. In fact, the results of our calculations show a large decrease in the T_1 energy upon substitution, 1.49 eV (833 nm) for Si–C_{60} compared with 1.63 eV (758 nm) for C_{60}. From this decrease in the $T_1 - S_0$ energy gap one can expect an increase in the T_1 nonradiative deactivation rate, as observed. The singlet and triplet transient absorption spectra show a shift to higher energy and a decrease in the extinction coefficients for Si–C_{60} compared with C_{60}, which is in agreement with previous reports on C_{60} derivatives.[17a]

The photophysical properties of Cu–cat along with several related catenates,[42] knots[43] and cage compounds[44] have been extensively investigated. The absorption bands in the UV region are due to ligand-centred (LC) ππ* transitions, whereas the much weaker absorption in the 390–700 nm spectral region is attributed to spin-allowed metal-to-ligand charge-transfer (MLCT) transitions.[45] Such transitions lie at low energy, as the Cu^+ ion is a good electron donor and the coordinated phenanthroline-type ligand has electron-accepting character. The low-energy, weak luminescence at room temperature originates from a couple of thermally equilibrated (singlet and triplet) MLCT levels[43, 45] (Figure 5). The associated excited-state lifetime in deaerated solution is 175 ns.

The rotaxane Si-C_{60}-Cu: Given the poor solubility of this compound, the determination of the molar absorption coefficients could not be performed. Interestingly, the profile of the absorption spectrum of Si-C_{60}-Cu cannot be superimposed very well on the sum of the absorption spectra of the model compounds expressed in ε units (note that the fullerene unit is present twice in the supramolecular structure; Figure 4), which seems to indicate some electronic interaction between the components. The anodic shift observed by cyclic voltammetry for the oxidation of the Cu^I centre of Si-C_{60}-Cu, with respect to Cu–cat and other analogous mononuclear complexes, could also be attributed to the strong electron-withdrawing effect of the two fullerene groups, which in turn could substantially destabilize the highest oxidation state of the Cu centre. However, we also believe that solvation effects resulting from the presence of the two fullerene moieties in the proximity of the metal centre are at the origin of the observed potential shift. In agreement with this proposal, the redox potential of the Si–C_{60} units is not affected in the supermolecule and the same holds for the energy of the singlet and triplet absorption bands (Figure 9, Tables 1 and 2). Also, all previous studies[6, 33] have shown that the methanobridge sp^3-C-atom in methanofullerenes efficiently blocks through-bond or through-space communications. Therefore, in our discussion we will assume that the single molecular components keep their own ground-state electronic properties while the detected changes in the photophysical properties of Si-C_{60}-Cu can be ascribed to the occurrence of intercomponent processes.

The most striking result concerning the photophysical properties of Si-C_{60}-Cu is that the excited-state properties observed in the model compounds Si–C_{60} and Cu–cat are strongly quenched. In particular we observe: a) quenching of the fullerene fluorescence; b) quenching of the MLCT emission; c) reduction in the yield and lifetime of the fullerene triplet; d) a large decrease in the photosensitization of singlet oxygen. Such observations clearly indicate the presence of novel competitive deactivation pathways in the excited states of Si-C_{60}-Cu with respect to the molecular components. The relevant rate constants can be calculated on the basis of Equation (1) where τ is the lifetime of a given (quenched) excited state in the supramolecular structure, and τ_0 is the (unquenched) lifetime of the same state in the model compound.

$$k = 1/\tau - 1/\tau_0 \qquad (1)$$

The construction of an energy level scheme for Si-C_{60}-Cu can be attempted on the basis of the spectroscopic and electrochemical data. In particular, to assign the excited-state energies of the single components in the supramolecular array Si-C_{60}-Cu, we took the luminescence maxima at 77 K of the corresponding components in Si-C_{60}-Cu or, if not available, of the reference model compounds. Accordingly, from Table 1, an energy of 1.73 eV for Si-$^1C_{60}$-Cu (the lowest excited singlet localized on Si–C_{60}) and 1.65 eV for the Si-C_{60}-*Cu (the MLCT manifold of singlet and triplet states localized on Cu–cat) were calculated. As we were unable to detect phosphorescence from Si-C_{60}-Cu and the model Si–C_{60}, we assume the energy of the Si-$^3C_{60}$-Cu state to take the calculated value of 1.49 eV (see above). In this type of approximate approach, the energy of the charge-separated state (Si-C_{60}^--Cu$^+$), formed by electron transfer from the metal to the fullerene, can be derived from the simple addition of the energy required to oxidize the Cu–cat moiety and to reduce the Si–C_{60} unit of the rotaxane in the same solvent (i.e., 1.46 eV from our electrochemical data). Finally an energy level diagram (Figure 12) is obtained in which all the levels appear very closely spaced in energy and the lowest ones are the triplet state Si-$^3C_{60}$-Cu and the charge-separated state Si-C_{60}^--Cu$^+$.

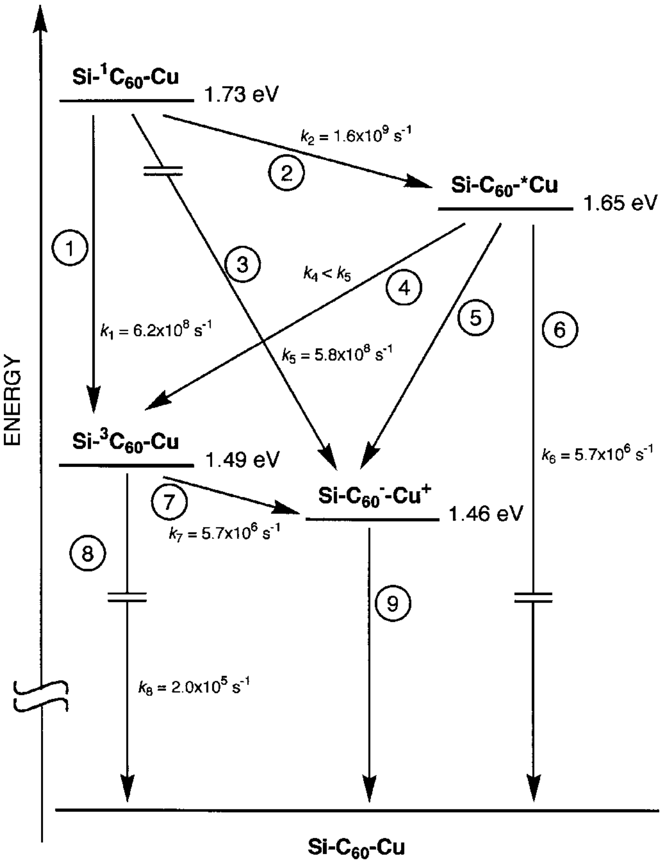

Figure 12. Energy-level diagram describing the intercomponent energy- and electron-transfer processes which occur in the rotaxane Si-C_{60}-Cu in CH_2Cl_2 solution. On the left the lowest electronic excited states centred on the fullerene stoppers are displayed and those centred on the Cu^I-complexed core on the right. Si-C_{60}-*Cu represents thermally equilibrated MLCT singlet and triplet states.

On the basis of this scheme the interpretation of our data is relatively simple. Excitation of Si-C_{60}-Cu at 355 or 532 nm leads to the population both of the fullerene-centred singlet excited state Si-$^1C_{60}$-Cu and of the Si-C_{60}-*Cu state in a 3:2 ratio, according to the absorption coefficients. Unfortunately, the emissions from these two levels occur in the same spectral region (Figure 5), but nevertheless the analysis of the luminescence decay at 700 nm reveals the presence of two different lifetimes, 0.5 and 1.7 ns, respectively (Figure 7). From the transient absorption data, we measured a lifetime of 0.4 ns for the fullerene singlet in Si-C_{60}-Cu while the triplet formation takes place on a longer timescale (1.8 ns; Figure 10). We therefore assign a lifetime of 0.45 ns (average of the emission and absorption data) to the singlet state of the fullerene unit in the rotaxane and the 1.7 ns lifetime to the Si-C_{60}-*Cu levels. A rate constant of 1.6×10^9 s^{-1} is derived for the step deactivating Si-$^1C_{60}$-Cu in the rotaxane [Eq. (1)]. At least two processes could be responsible for the quenching of the fullerene-centred singlet, namely energy transfer to the MLCT singlet of the Cu^I-complexed core ($\Delta G^0 = -0.08$ eV; step 2; Figure 12), or electron transfer to give the charge-separated state ($\Delta G^0 = -0.27$ eV; step 3).

Energy transfer (step 2) may occur by two different mechanisms: the Förster-type mechanism,[46] based on coulombic interactions, and the Dexter-type mechanism,[47] based on an exchange interaction. The first case does not require contact between the partners, while the latter requires an overlap of orbitals, possibly mediated by other interposed chemical bonds; put simply, it can be visualized as a simultaneous double electron exchange between the donor and the acceptor.

The rate of energy transfer according to a Förster-type mechanism can be calculated from spectroscopic quantities and turns out to be 2×10^6 s^{-1},[48] well below the experimental rate k_2. We can therefore exclude the possibility that the deactivation of the fullerene localized singlet state is due to this type of process.

In view of the approximate approach applied here, we will not enter into a detailed discussion about the other possible mechanism, namely energy transfer by means of electron exchange or electron transfer, but rather try to discuss it in qualitative terms. The larger driving force of electron transfer (step 3; $\Delta G^0 = -0.27$) compared with energy transfer (step 2; $\Delta G^0 = -0.08$) is largely compensated by the much higher reorganization energy involved in the former process, in which a net charge transfer occurs. Furthermore, we do not have any spectroscopic evidence for the formation of the charge-separated state on this timescale (see below). On the basis of these considerations, we would assign the observed quenching rate of the singlet fullerene moiety in Si-C_{60}-Cu to an energy transfer by an electron exchange mechanism to the MLCT manifold of the Cu^I-complexed moiety (step 2; Figure 12).[49]

Following the decay of the fullerene singlet, which occurs in part by energy transfer and in part by intersystem crossing (28%, according to the ratio $k_1/k_1 + k_2$), the Cu^I-complexed unit is quenched from 175 ns to 1.7 ns lifetime with a rate of 5.8×10^8 s^{-1}. The possible deactivating pathways for the MLCT manifold are: i) energy transfer to the fullerene localized triplet (step 4; $\Delta G^0 = -0.16$ eV) and ii) electron transfer to the charge-separated state (step 5; $\Delta G^0 = -0.19$ eV). The transient absorption data concerning the evolution of the fullerene triplet Si-$^3C_{60}$-Cu indicate that only a negligible part of the observed triplet is formed by the process displaying the lifetime of $\tau = 1.8$ ns (Figure 10), which is in close agreement with the second luminescence decay with a 1.7 ns lifetime monitored for Si-C_{60}-*Cu (Figure 7). Since under our experimental conditions 40% of the absorbed photons produces the Cu^I-complex-centred MLCT excited state directly, we would expect a larger contribution of fullerene triplet formation than actually observed if step 4 is to be efficient. Therefore, we would tend to ascribe the rate constant of deactivation of the MLCT levels ($k_5 = 5.8 \times 10^8\,s^{-1}$) mainly to electron transfer leading to the charge-separated state (step 5). It should be noted that in step 5 the less favourable ΔG^0 for electron transfer ($\Delta G^0 = -0.19$ eV) with respect to step 3 ($\Delta G^0 = -0.27$ eV) can be counterbalanced by the fact that the electron has to be moved over a shorter distance. In fact in both cases it has to migrate to a fullerene unit, but starting from the central metal in step 3 and from the phenanthroline ligand in step 5 (in MLCT excited states, the electron is localized on the ligand).[50] The overall experimental yield of triplet formation in Si-C_{60}-Cu (about 30%), compared with the reference compound Si–C_{60}, is in very good agreement with the calculated value (28%, vide supra). This close agreement between experimental and calculated yields confirms that only a negligible fraction of triplet is produced via step 4. Finally, the triplet is also quenched, as we can confirm from the lifetime of this state, which changes from 5 μs in Si–C_{60} to 170 ns in Si-C_{60}-Cu. Both the decreases in lifetime and yield of formation are reflected by the reduced ability of Si-C_{60}-Cu to sensitize singlet-oxygen luminescence (Table 2). The quenching of the fullerene-centred triplet ($k_7 = 5.7 \times 10^6\,s^{-1}$) can only be assigned to the charge separation step 7, which is a slightly exergonic pathway ($\Delta G^0 \approx -0.03$ eV).

Clearcut evidence of Si-C_{60}^--Cu$^+$ state formation cannot be derived from our transient absorption spectra. The presence of the oxidized transient species $[Cu(phen)_2]^{2+}$ is barely perceptible as it is expected to display only very weak and broad absorption features ($\varepsilon_{max} \approx 10^2\,M^{-1}cm^{-1}$) above 400 nm,[51] whereas anions of C_{60} and its derivatives are reported to display typical absorption bands around 950 and over 1000 nm.[52] Some authors have also assigned an absorption band around 750 nm to C_{60}^-.[17g] In the picosecond absorption experiment, where a maximum time window of 3 ns can be probed, we did not observe any signals in the 900–1050 nm region after the decay of the Si-$^1C_{60}$-Cu excited state and this gives further support to the assignment of the decay of such a state to energy rather than electron transfer (Figure 12). Our nanosecond flash photolysis apparatus does not allow measurements over 850 nm, but a very weak absorption around 740 nm ($A = 0.006$) was recorded after the decay of the triplet. The lifetime of this species in air-purged solution is 1.7 μs. If this species were assigned as the charge-separated state we could attempt to determine the yield of charge separation. The absorption coefficient ε of the C_{60} anion at 750 nm can be calculated to be approximately $3 \times 10^3\,M^{-1}cm^{-1}$.[17g] By taking $^3C_{60}$ as a standard with $\Phi_T = 1$ and $\varepsilon = 2 \times 10^4\,M^{-1}cm^{-1}$ at 750 nm,[5] an overall yield of charge separation of the order of 20% can be derived from our data (Figure 11). The most surprising fact is, however, the quite long lifetime of this supposed charge-separated state ($\tau = 1.7$ μs), which would imply extremely unfavourable conditions for the back-electron-transfer reaction (step 9). Very few cases of long-living (microsecond timescale) charge-separated states for C_{60}-based dyads have been reported so far and those only in polar solvents.[17d, 17i]

In an approximate approach a long lifetime of the charge-separated state, that is a low rate of back electron transfer, would require that both of the following conditions are met: i) the ΔG^0 of the reaction is well above the reorganization energy λ, to place it in the Marcus inverted region[53] where the rate of electron transfer is expected to decrease by increasing the driving force; ii) the electronic interaction among the components (fullerene and Cu^I-complex units) is negligible.[54] None of the former conditions appear to be met: the calculated reorganizational energy for the electron-transfer process is about 1.2 eV,[55] while the electronic term is sizeable as some coupling of the components is apparent even from the spectroscopic data (vide supra). Even making allowances for the approximate treatment used, the expected rate of back electron transfer is definitely several orders of magnitude higher than the experimental one. This is in agreement with most of the current literature on C_{60}-based dyads,[17] which reports poor yields and short lifetimes (picosecond timescale) for charge-separated states in nonpolar solvents. In the absence of further experimental evidence, we cannot assign the intermediate detected at 740 nm with 1.7 μs lifetime to a charge-separated state, especially in view of the fact that only 2–3% of any unquenched fullerene derivative present as an impurity would give a similar absorbance.

The lack of evidence for the charge-separated state is most likely the result of an extremely fast charge-recombination process that prevents its accumulation. This is in agreement with the above-reported considerations on the rate of such back-electron-transfer processes.

Conclusions

The synthesis of the first supramolecular rotaxane system containing fullerene and $[Cu(phen)_2]^+$-type molecular units has been reported. These components were chosen because one could expect them to be able to give photoinduced electron transfer from the Cu^I-complexed core to the fullerene stoppers. The photophysical investigations have shown that excited-state intercomponent processes take place. In particular, all the excited states of the molecular components are deactivated by means of a sequence of energy and electron-transfer steps to a low-energy, charge-separated state which is made available. Direct evidence for the charge-separated state is lacking, probably because it does not accumulate in solution as a result of the fact that the back-electron-transfer reaction is faster than the forward process. Nevertheless, clear indication of its involvement comes from the quenching of the triplet state Si-$^3C_{60}$-Cu and from the lack of singlet-oxygen sensitization. The molecular components assembled in Si-C_{60}-Cu prove to be useful buiding blocks for the construction of supermolecules capable of performing photoinduced electron transfer, especially since they are extremely stable under high-energy, long-duration laser irradiation. Their assembly in rigid supramolecular systems with longer, well-defined intercomponent distances is expected to promote long-lived charge separations. We are currently working along these lines.

Experimental Section

Synthesis: Reagents and solvents were purchased at reagent grade and used without further purification. CH_2Cl_2 was distilled over CaH_2. C_{60} was isolated from the commercially available C_{60}/C_{70} mixture according to a previously reported method.[56] Compounds **1**,[27] **2**[30] and Si – C_{60} [27] were prepared as previously reported. Melting points were measured on a Büchi apparatus and are uncorrected. IR spectra were measured on a Perkin – Elmer 580 instrument. NMR spectra were recorded on a Bruker AM500 and on a Varian Gemini300 at 296 or 300 K, with solvent peaks as reference. Mass spectra were measured on a VG ZAB 2SEQ instrument (FAB).

Si-C_{60}-Cu and 3: A mixture of CuCl (1.58 g, 16 mmol) and TMEDA (1.86 g, 16 mmol) in CH_2Cl_2 (100 mL) was added to a mixture of **2** (71 mg, 0.064 mmol), **1** (291 mg, 0.31 mmol, 4.8 equiv) and 4 Å molecular sieves (5 g) in CH_2Cl_2 (700 mL). The resulting dark green mixture was stirred vigorously under dry air for 16 h. The CH_2Cl_2 solution was then filtered to remove the molecular sieves, washed with water (4 × 200 mL) and treated overnight with a large excess of potassium tetrafluoroborate in a minimum of water (anion exchange). The organic layer was washed with water (2 × 200 mL), dried ($MgSO_4$), filtered and evaporated to dryness. Column chromatography on silica gel yielded the bisfullerene derivative **3** (eluent CH_2Cl_2) and the copper(I) complex Si-C_{60}-Cu (eluent CH_2Cl_2, containing 5 – 7 % MeOH). An analytical sample of Si-C_{60}-Cu (28.7 mg, 0.01 mmol, 15 % yield) was obtained by crystallization from CS_2/hexane, whereas pure **3** (60 mg, 0.032 mmol, 20 % yield) was isolated after further column chromatography on silica gel (eluent cyclohexane) followed by recrystallization from CS_2/pentane.

Si-C_{60}-Cu: Dark red solid; m.p. > 280 °C; IR ($CHCl_3$): $\tilde{\nu} = 2944$ (s), 2866 (s), 2167 (w), 1600 (s), 1489 (s), 1239 (s), 1172 (m), 1094 (m), 1011 (m), 828 (m) cm^{-1}; ^1H NMR ($CDCl_3$/CS_2, 1:1, 300 MHz): $\delta = 1.18$ (s, 42 H), 3.19 (m, 4 H), 3.57 (m, 4 H), 3.84 (m, 4 H), 3.92 (m, 4 H), 4.68 (s, 4 H), 5.81 (d, $J = 8.0$ Hz, 4 H), 6.19 (d, $J = 8.5$ Hz, 4 H), 6.87 (d, $J = 8.5$ Hz, 4 H), 7.48 (d, $J = 8.0$ Hz, 4 H), 7.96 (m, 4 H), 8.15 (s, 2 H), 8.30 (s, 2 H), 8.65 (d, $J = 8.5$ Hz, 2 H), 8.91 (d, $J = 8.5$ Hz, 2 H); ^{13}C NMR ($CDCl_3$/CS_2, 1:1, 125.8 MHz): $\delta =$ 11.45, 18.82, 29.30, 56.15, 67.50, 68.92, 69.45, 71.29, 71.40, 71.52, 73.15, 74.93, 75.21, 88.76, 96.94, 113.20, 113.35, 116.31, 123.89, 124.50, 126.24, 127.12, 127.60, 128.28, 128.83, 129.40, 130.80, 132.48, 133.70, 136.78, 138.95, 139.12, 139.40, 141.19, 141.25, 142.11, 142.17, 142.38, 142.90, 142.95, 143.01, 143.08, 143.11, 143.16, 143.17, 144.02, 144.06, 144.48, 144.71, 144.75, 144.81, 144.94, 145.07, 145.20, 145.35, 145.42, 145.44, 145.47, 145.51, 145.59, 155.21, 157.47, 157.62, 158.94; MS (FAB, *m*-nitrobenzyl alcohol): *m*/*z* (%): 2900.2 (100) $[M - BF_4]^+$, 2179.7 (14) $[M - BF_4 - C_{60}]^+$.

3: Black crystals; m.p. > 280 °C; UV/Vis, ^1H and ^{13}C NMR, and mass spectra identical to those of an authentic sample previously prepared by another method.[27]

Electrochemical measurements

Solvents and supporting electrolytes: CH_2Cl_2 (spectroscopic grade) was distilled over CaH_2 under argon and stored under argon. The supporting electrolyte, $nBu_4N^+BF_4^-$, was recrystallized twice from ethanol/water and thoroughly dried in vacuo over P_2O_5.

Instrumentation: A Bruker EI30M potentiostat and an Ifelec IF3802 recorder were used for cyclic voltammetry measurements. A saturated calomel electrode (SCE) served as the reference electrode. It was separated from the test solution by an auxiliary compartment filled with a 10^{-1} M solution of $nBu_4N^+BF_4^-$ in CH_2Cl_2. The working electrode was planar platinum. All experiments were done under an argon atmosphere in a Metrohm universal recipient, in a three-electrode configuration.

Spectroscopic and photophysical measurements: For solubility reasons, all the spectroscopic investigations were carried out in CH_2Cl_2 (Carlo Erba, spectrofluorimetric grade). In this solvent, Cu – cat and Si – C_{60} are readily soluble, C_{60} is very slowly soluble (the dissolution of 1 mg in 10 cm^3 of solvent takes several days), and Si-C_{60}-Cu is poorly soluble. To obtain transparent solutions of Si-C_{60}-Cu filtration is necessary, thus making the determination of the molar absorption coefficients impossible. The samples were placed in fluorimetric 1 cm path cuvettes and, when necessary, purged of oxygen with argon. For any quantitative determination on the supramolecular species Si-C_{60}-Cu, we have taken into account the partition of the light (3:2 ratio fullerene:Cu^I-based moiety), both at 355 and at 532 nm, on the basis of the molar extinction coefficients of the reference compounds Si – C_{60} and Cu – cat.

Absorption spectra were recorded with a Perkin – Elmer λ5 spectrophotometer. Uncorrected emission spectra were obtained with a Spex Fluorolog II spectrofluorimeter (continuous Xe lamp), equipped with a Hamamatsu R-928 photomultiplier tube. Fluorescence quantum yields were measured with the method described by Demas and Crosby[57] with $[Os(phen)_3]^{2+}$ in acetonitrile as a standard ($\Phi = 0.005$).[58] The attempts to detect delayed luminescence spectra of fullerene triplets were carried out both with the Spex Fluorolog II with a pulsed Xe lamp (1934D Phosphorimeter) and with a Perkin – Elmer LS-50 spectrofluorimeter (pulsed Xe lamp) equipped with a red-enhanced photomultiplier (Hamamatsu R-3896).

Emission lifetimes in the nanosecond timescale were determined with IBH single-photon counting equipment (N_2 lamp, $\lambda_{exc} = 337$ nm, 1 ns time resolution). For picosecond time resolution, a fluorimeter based on a single-shot streak camera (Hamamatsu C1587) and a Nd-YAG laser (PY62-10 Continuun) with a 35 ps pulse was used; the system is described in more detail elsewhere.[59] The excitation wavelength was 532 nm and the energy was 1 – 2 mJ; 1000 to 2000 laser shots were accumulated to obtain the streak images; time profiles were obtained by selecting 20 nm intervals around the emission maxima.

Transient absorption spectra and lifetimes with picosecond time resolution were obtained with a pump and probe system based on the 35 ps Nd:YAG laser (see above) and an OMA detector. Excitation with the second harmonic (532 nm) at 4 – 7 mJ per pulse was used. Details of this photolysis system have been already reported.[60]

The nanosecond transient absorption spectra were recorded by means of the third harmonic (355 nm) of a Nd:YAG laser (JK Lasers) with 20 ns pulse and 1 – 2 mJ per pulse. The details of the flash photolysis system are reported elsewhere.[61] The second harmonic (532 nm) of the same Nd:YAG laser was also used in the experiments for the detection of sensitized singlet oxygen, whose IR luminescence ($\lambda_{max} = 1269$ nm) was collected perpendicular to the excitation in close proximity to the sample cell by an unbiassed Ge photodiode (Judson J16-5). A silicon metal filter (II – VI Inc.), with a band-pass $\lambda > 1100$ nm, placed in front of the detector prevented the laser harmonics and sample emission from reaching the detector. The photodetector output was fed across a load resistance of 240 Ω into a R7912 Transient Digitizer equipped with a 7A22 vertical differential amplifier, operated at 0.3 MHz band-pass. The time resolution of the system was a few microseconds. The relative yield was obtained by comparing the singlet-oxygen luminescence signal extrapolated to zero time ($\tau \approx 100$ μs) of solutions displaying the same absorbances at 532 nm ($A = 0.14$).

Experimental uncertainties are estimated to be ± 8 % for lifetime determination, ± 20 % for quantum yields and ± 3 nm for emission and absorption peaks.

All the experiments were performed at 293 K, unless otherwise specified.

Acknowledgments: This research was supported by the Italian CNR (Progetto Strategico Tecnologie Chimiche Innovative), the French CNRS, the Swiss National Science Foundation, the EU (TMR, grant no. FMRX-CT96-0031), and NATO (Supramolecular Chemistry Special Programme, grant no. CRG 951279). J.-F.N. thanks the EU for a post-doctoral fellowship (Human Capital and Mobility). FRAE authors thank M. Minghetti and L. Ventura for technical assistance.

Received: June 20, 1997 [F735]

[1] H. W. Kroto, J. R. Heath, S. C. O'Brien, R. F. Curl, R. E. Smalley, *Nature (London)* **1985**, *318*, 162–163.

[2] a) R. Taylor, D. Walton, *Nature (London)* **1993**, *363*, 685–693; b) A. Hirsch, *The Chemistry of the Fullerenes*, Thieme, Stuttgart, **1994**; c) F. Diederich, C. Thilgen, *Science (Washington D.C.)* **1996**, *271*, 317–323.

[3] a) F. Diederich, R. L. Whetten, *Acc. Chem. Res.* **1992**, *25*, 119–126; b) C. Thilgen, A. Herrmann, F. Diederich, *Angew. Chem.* **1997**, *109*, 2362–2374; *Angew. Chem. Int. Ed. Engl.* **1997**, *36*, 2268-2280.

[4] a) W. Marx, H. Schier, in *Fullerenes and Fullerene Nanostructures* (Eds: H. Kuzmany, J. Fink, M. Mehring, S. Roth), World Scientific, Singapore, **1996**, p. 633; b) T. Braun, E. Osawa, *Fullerene Sci. Technol.* **1996**, *4(6)*, iv.

[5] C. S. Foote, *Top. Curr. Chem.* **1994**, *169*, 347–363.

[6] a) T. Suzuki, Y. Maruyama, T. Akasaka, W. Ando, K. Kobayashi, S. Nagase, *J. Am. Chem. Soc.* **1994**, *116*, 1359–1363; b) C. Boudon, J.-P. Gisselbrecht, M. Gross, L. Isaacs, H. L. Anderson, R. Faust, F. Diederich, *Helv. Chim. Acta* **1995**, *78*, 1334-1344; c) Q. Xie, E. Pérez-Cordero, L. Echegoyen, *J. Am. Chem. Soc.* **1992**, *114*, 3978–3980; d) P.-M. Allemand, G. Srdanov, A. Koch, K. Khemani, F. Wudl, Y. Rubin, F. Diederich, M. M. Alvarez, S. J. Anz, R. L. Whetten, *ibid.* **1991**, *113*, 2780–2781.

[7] a) H. Ajie, M. M. Alvarez, S. J. Anz, R. D. Beck, F. Diederich, K. Fostiropoulos, D. R. Huffman, W. Krätschmer, Y. Rubin, K. E. Schiver, D. R. Sensharma, R. L. Whetten, *J. Phys. Chem.* **1990**, *94*, 8630–8634; b) J. P. Hare, H. W. Kroto, R. Taylor, *Chem. Phys. Lett.* **1991**, *177*, 394–398; c) S. Leach, M. Vervloet, A. Desprès, E. Bréheret, J. P. Hare, T. J. Dennis, H. W. Kroto, R. Taylor, D. R. M. Walton, *Chem. Phys.* **1992**, *160*, 451–466.

[8] a) A. Watanabe, I. Osamu, M. Watanabe, H. Saito, M. Koishi, *Chem. Commun.* **1996**, 117–118; b) T. W. Ebbesen, K. Tanigaki, S. Kuroshima, *Chem. Phys. Lett.*, **1991**, *181*, 501–504.

[9] a) R. J. Sension, C. M. Phillips, A. Z. Szarka, W. J. Romanow, A. R. McGhie, J. P. McCauley, Jr., A. B. Smith III, R. M. Hochstrasser, *J. Phys. Chem.* **1991**, *95*, 6075–6078; b) N. M. Dimitrijevic, P. V. Kamat, *ibid.* **1992**, *96*, 4811–4814.

[10] a) D. Kim, M. Lee, Y. D. Suh, S. K. Kim, *J. Am. Chem. Soc.* **1992**, *114*, 4429–4430; b) J. Catalán, J. Elguero, *ibid.* **1993**, *115,* 9249–9252.

[11] a) S. P. Sibley, S. M. Argentine, A. H. Francis, *Chem. Phys. Lett.* **1992**, *188*, 187–193; b) K. Palewka, J. Sworakowski, H. Chojnacki, E. C. Meister, U. P. Wild, *J. Phys. Chem.* **1993**, *97,* 12167—12172; c) W. C. Hung, C. D. Ho, C. P. Liu, Y. P. Lee, *ibid.* **1996**, *100,* 3927–3932; d) Y. Zeng, L. Biczok, H. Linschitz, *ibid.* **1992**, *96,* 5237–5239; e) D. J. van der Heuvel, Y. I. Chan, E. J. J. Groenen, J. Schmidt, J. Meijer, *Chem. Phys. Lett.* **1994**, *231*, 111–118.

[12] J. W. Arbogast, A. O. Darmanyan, C. S. Foote, Y. Rubin, F. Diederich, M. M. Alvarez, S. J. Anz, R. L. Whetten, *J. Phys. Chem.* **1991**, *95*, 11–12.

[13] R. R. Hung, J. J. Grabowski, *J. Phys. Chem.* **1991**, *95*, 6073–6075.

[14] a) D. Dubois, K. M. Kadish, *J. Am. Chem. Soc.* **1991**, *113*, 4364–4366; b) F. Paolucci, M. Marcaccio, S. Roffia, G. Orlandi, F. Zerbetto, M. Prato, M. Maggini, G. Scorrano, *J. Am. Chem. Soc.* **1995**, *117*, 6572–6580.

[15] See for example: a) J. W. Arbogast, C. S. Foote, M. Kao, *J. Am. Chem. Soc.* **1992**, *114*, 2277–2279; b) Y. P. Sun, C. E. Bunker, B. Ma, *ibid.* **1994**, *116*, 9692–9699; c) J. P. Mittal, *Pure Appl. Chem.* **1995**, *67*, 103–110; d) O. Ito, Y. Sazaki, Y. Yashikawa, A. Watanabe, *J. Phys. Chem.* **1995**, *99*, 9398–9842; e) C. A. Steren, H. van Willingen, L. Biczók, N. Gupta, H. Luishito, *ibid.* **1996**, *100*, 8920–8926.

[16] a) N. S. Sariciftci, L. Smilowitz, A. J. Heeger, F. Wudl, *Science (Washington D.C.)* **1992**, *2589*, 1474–1476; b) A. Watanabe, O. Ito, *J. Chem. Soc. Chem. Commun.* **1994**, 1285–1286; c) A. Watanabe, O. Ito, *J. Phys. Chem.* **1994**, *98*, 7736–7740.

[17] a) P. Liddell, A. N. Macpherson, J. Sumida, L. Demanche, A. L. Moore, T. A. Moore, D. Gust, *Photochem. Photobiol.* **1994**, *60*, 537–541; b) R. M. Williams, J. M. Zwier, J. W. Verhoeven, *J. Am. Chem. Soc.* **1995**, *117*, 4093–4099; c) H. Imahori, S. Cardoso, D. Tatman, S. Lin, L. Noss, G. R. Seely, L. Sereno, J. Chessa de Silber, T. A. Moore, A. L. Moore, D. Gust, *Photochem. Photobiol.* **1995**, *62*, 1009–1014; d) N. S. Sariciftci, F. Wudl, A. J. Heeger, M. Maggini, G. Scorrano, M. Prato, J. Bourassa, P. C. Ford, *Chem. Phys. Lett.* **1995**, *247*, 510–514; e) D. Kuciauskas, S. Lin, G. R. Seely, A. L. Moore, T. A. Moore, D. Gust, T. Drovetskaya, C. A. Reed, P. D. W. Boyd, *J. Phys. Chem.* **1996**, *100*, 15926—15932; f) H. Imahori, K. Hagiwara, M. Aoki, T. Akiyama, S. Taniguchi, T. Okada, T. Shirakawa, Y. Sakata, *J. Am. Chem. Soc.* **1996**, *118*, 11771–11782; g) R. M. Williams, M. Koeberg, J. M. Lawson, Y.-Z. An, Y. Rubin, M. N. Paddon-Row, J. W. Verhoeven, *J. Org. Chem.* **1996**, *61*, 5055–5062; h) D. Armspach, E. C. Constable, F. Diederich, C. E. Housecroft, J.-F. Nierengarten, *Chem. Commun.* **1996**, 2009–2010; i) D. M. Guldi, M. Moggini, G. Scorrano, M. Prato, *J. Am. Chem. Soc.* **1997**, *119*, 974–980; j) P. A. Liddell, D. Kucianscas, J. P. Sumide, B. Nash, O. Nguyen, A. Moore, T. A. Moore, D. Gust, *ibid.* **1997**, *119*, 1400–1405; k) T. D. M. Bell, T. A. Smith, K. P. Ghiggino, M. G. Ranasinghe, M. G. Shephard, M. N. Paddon-Row, *Chem. Phys. Lett.* **1997**, *268*, 223–228.

[18] a) *The Reaction Center of Photosynthetic Bacteria* (Ed.: M.-E. Michel-Beyerle), Springer, Berlin, **1995**; b) J. Barber, B. Anderson, *Nature (London)* **1994,** *370*, 31–34.

[19] a) *Molecular Electronic Devices* (Eds.: F. L. Carter, R. E. Siatowski, H. Woltjen), North Holland, Amsterdam, **1988**; b) V. Balzani, F. Scandola, *Supramolecular Photochemistry*, Ellis Horwood, Chichester (UK), **1991**, chapter 12.

[20] a) B. O'Regan, M. Grätzel, *Nature (London)* **1991**, *353*, 737–740; b) M. Grätzel, *Comments Inorg. Chem.* **1991**, *12*, 93–111; c) C. A. Bignozzi, R. Argazzi, C. Chiorboli, F. Scandola, B. R. Dyer, J. R. Schoonover, T. J. Meyer, *Inorg. Chem.* **1994**, *33*, 1652–1659; d) V. Balzani, F. Scandola, in *Comprehensive Supramolecular Chemistry*, *Vol. 10* (Ed.: D. N. Reinhoudt), Pergamon, Oxford, **1996**; p. 1.

[21] a) R. A. Bissel, A. P. De Silva, H. Q. N. Gunaratne, P. L. M. Lynch, G. E. M. Maguire, C. P. McCoy, K. R. A. S. Sandanayake, *Top. Curr. Chem.* **1993**, *168*, 223–264; b) L. Fabbrizzi, A. Poggi, *Chem. Soc. Rev.* **1995**, 197–202; c) A. P. De Silva, C. P. McCoy, *Chem. Ind. (London)* **1994**, *24*, 992–996.

[22] a) M. R. Wasielewski, M. P. O'Neil, D. Gosztola, M. P. Niemczyk, W. A. Svec, *Pure Appl. Chem.* **1992**, *64*, 1319–1325; b) S. L. Gilat, S. M. Kawai, J.-M. Lehn, *Chem. Eur. J.* **1995**, *1*, 275–284.

[23] a) B. T. Ahn, D. R. McMillin, *Inorg. Chem.* **1978**, *17*, 2253–2258; b) N. Alonso-Vante, V. Ern, P. Chartier, C. O. Dietrich-Buchecker, D. R. McMillin, P. A. Marnot, J.-P. Sauvage, *Nouv. J. Chim.* **1983**, *7*, 3–5; c) A. Edel, P. A. Marnot, J.-P. Sauvage, *ibid.* **1986**, *8*, 495–498; d) N. Alonso-Vante, J.-F. Nierengarten, J.-P. Sauvage, *J. Chem. Soc. Dalton Trans.* **1994**, 1649–1654.

[24] a) C. C. Phifer, D. R. McMillin, *Inorg. Chem.* **1986**, *25*, 1329–1333; b) A. K. Ichinaga, J. R. Kirchhoff, D. R. McMillin, C. O. Dietrich-Buchecker, P. A. Marnot, J.-P. Sauvage, *ibid.* **1987**, *26*, 4290–4292; c) A. K. Gushurst, D. R. McMillin, C. O. Dietrich-Buchecker, J.-P. Sauvage, *ibid.* **1989**, *28*, 4070–4072.

[25] J.-C. Chambron, C. O. Dietrich-Buchecker, J.-P. Sauvage, in *Comprehensive Supramolecular Chemistry*, *Vol. 9* (Ed.: J.-M. Lehn), Pergamon, Oxford, **1996**, p. 43.

[26] For a preliminary communication of the synthesis of Si-C$_{60}$-Cu see: F. Diederich, C. Dietrich-Buchecker, J.-F. Nierengarten, J.-P. Sauvage, *J. Chem. Soc. Chem. Commun.* **1995**, 781–782.

[27] a) H. L. Anderson, R. Faust, Y. Rubin, F. Diederich, *Angew. Chem.* **1994**, *106*, 1427–1429; *Angew. Chem. Int. Ed. Engl.* **1994**, *33*, 1366–1368; b) P. Timmerman, H. L. Anderson, R. Faust, J.-F. Nierengarten, T. Habicher, P. Seiler, F. Diederich, *Tetrahedron* **1995**, *52*, 4925–4947; c) P. Timmerman, L. E. Witschel, F. Diederich, *Helv. Chim. Acta* **1996**, *79*, 6–20.

[28] N. Armaroli, V. Balzani, L. De Cola, J.-P. Sauvage, C. O. Dietrich-Buchecker, J.-M. Kern, A. Bailal, *J. Chem. Soc. Dalton Trans.* **1993**, 3241–3247.

[29] a) Y.-Z. An, G. A. Ellis, A. L. Viado, Y. Rubin, *J. Org. Chem.* **1995**, *60*, 6353–6361; b) K. Komatsu, N. Takimoto, Y. Murata, T. S. M. Wan, T. Wong, *Tetrahedron Lett.* **1996**, *37*, 6153–6156; c) Y. Murata, K. Motayama, K. Komatsu, T. S. M. Wan, *Tetrahedron* **1996**, *52*, 5077–5090.

[30] a) C. O. Dietrich-Buchecker, A. Khemiss, J.-P. Sauvage, *J. Chem. Soc. Chem. Commun.* **1986**, 1376–1378; b) C. O. Dietrich-Buchecker, C. Hemmert, A. Khemiss, J.-P. Sauvage, *J. Am. Chem. Soc.* **1990**, *112*, 8002–8008.

[31] A. S. Hay, *J. Org. Chem.* **1962**, *27*, 3320–3321.

[32] P. Federlin, J.-M. Kern, A. Rastegar, C. O. Dietrich-Buchecker, P. A. Marnot, J.-P. Sauvage, *New J. Chem.* **1990**, *14*, 9–12.

[33] a) T. Suzuki, Q. Li, K. C. Khemani, F. Wudl, O. Almarsson, *Science (Washington D.C.)* **1992**, *254*, 1186–1188; b) T. Suzuki, Q. Li, K. C. Khemani, F. Wudl, Ö. Almarsson, *J. Am. Chem. Soc.* **1992**, *114,* 7300–7301; c) M. Eiermann, F. Wudl, M. Prato, M. Maggini, *ibid.* **1994**, *116*, 8364–8365.

[34] a) H. L. Anderson, C. Boudon, F. Diederich, J.-P. Gisselbrecht, M. Gross, P. Seiler, *Angew. Chem.* **1994**, *106*, 1691–1694; *Angew. Chem. Int. Ed. Engl.* **1994**, *33*, 1628–1631; b) F. Diederich, J.-F. Nierengarten, P. Timmerman, C. Boudon, J.-P. Gisselbrecht, M. Gross, unpublished results.

[35] M. R. Wasielewski, M. O'Neil, K. R. Lykke, M. J. Pellin, D. M. Gruen, *J. Am. Chem. Soc.* **1991**, *113*, 2774–2776.

[36] a) A. Vasella, P. Uhlmann, C. A. A. Waldraff, F. Diederich, C. Thilgen, *Angew. Chem.* **1992**, *104*, 1383–1385; *Angew. Chem. Int. Ed. Engl.* **1992**, *31*, 1388–1390; b) F. Diederich, U. Jonas, V. Gramlich, A. Herrmann, H. Ringsdorf, C. Thilgen, *Helv. Chim. Acta* **1993**, *76*, 2445–2453.

[37] N. Armaroli, M. A. J. Rodgers, P. Ceroni, V. Balzani, C. O. Dietrich-Buchecker, J.-M. Kern, A. Bailal, J.-P. Sauvage, *Chem. Phys. Lett.* **1995**, *241*, 555–558.

[38] J. L. Anderson, Y.-Z. An, Y. Rubin, C. S. Foote, *J. Am. Chem. Soc.* **1994**, *116*, 9763–9764.

[39] W. P. Anderson, W. D. Edwards, C. S. Zerner, *Inorg. Chem.* **1986**, *25*, 2728–2732.

[40] A. D. Bacon, M. C. Zerner, *Theor. Chim. Acta* **1979**, *53*, 21–51.

[41] A. Bianco, M. Maggini, G. Scorrano, C. Toniolo, G. Marconi, C. Villani, M. Prato, *J. Am. Chem. Soc.* **1996**, *118*, 4072–4080.

[42] a) N. Armaroli, V. Balzani, F. Barigelletti, L. De Cola, J.-P. Sauvage, C. Hemmert, *J. Am. Chem. Soc.* **1991**, *113*, 4033–4035; b) N. Armaroli, V. Balzani, F. Barigelletti, L. De Cola, L. Flamigni, J.-P. Sauvage, C. Hemmert, *ibid.* **1994**, *116*, 5211–5217; c) N. Armaroli, V. Balzani, L. De Cola, J.-P. Sauvage, C. Hemmert, *New J. Chem.* **1994**, *18*, 775–782; d) J.-M. Kern, J.-P. Sauvage, J.-L. Weidmann, N. Armaroli, L. Flamigni, P. Ceroni, V. Balzani, *Inorg. Chem.* **1997**, *36*, 5329–5338.

[43] a) C. O. Dietrich-Buchecker, J.-F. Nierengarten, J.-P. Sauvage, N. Armaroli, V. Balzani, L. De Cola, *J. Am. Chem. Soc.* **1993**, *115*, 11237–11244; b) C. O. Dietrich-Buchecker, J.-P. Sauvage, N. Armaroli, P. Ceroni, V. Balzani, *Angew. Chem.* **1996**, *108*, 1190–1193; *Angew. Chem. Int. Ed. Engl.* **1996**, *35*, 1119–1121.

[44] F. Vögtle, I. Lüer, V. Balzani, N. Armaroli, *Angew. Chem.* **1991**, *103*, 1367–1368; *Angew. Chem. Int. Ed. Engl.* **1991**, *30*, 1333–1336.

[45] R. M. Everly, D. R. McMillin, *J. Phys. Chem.* **1991**, *95*, 9071–9075, and references therein.

[46] T. Förster, *Discuss. Faraday Soc.* **1959**, *27*, 7–17.

[47] D. L. Dexter, *J. Chem. Phys.* **1953**, *21*, 836–850.

[48] The energy transfer rate was calculated according to: $k = [(8.8 \times 10^{-25} K^2 \Phi)/(n^4 \tau r^6)] J_F$ where Φ and τ are the luminescence quantum yield and lifetime of the $Si-C_{60}$ excited state, n is the refractive index of CH_2Cl_2, r is the centre–centre distance (through space) of $Si-C_{60}$ and the Cu–cat complex in the rotaxane, taken as 14 Å. The geometric factor K^2, which depends on the relative orientation of the dipoles and can vary in the range 0–4, is assumed to be 2/3 and corresponds to a statistical orientation. The overlap integral J_F[46] is calculated from the spectroscopic data of $Si-C_{60}$ emission and Cu–cat absorption coefficients and is 3.6×10^{-16} cm^3 M^{-1}.

[49] The rate of energy transfer occurring by a Dexter mechanism can be expressed as $k = (4\pi^2 H^2) J_D / h$ (Oevering et al., *Chem. Phys. Lett.* **1988**, *143*, 488–495). When the experimental rate and the overlap integral calculated from the spectroscopic data were introduced,[47] $J_D = 4.6 \times 10^{-5}$ cm, the calculated interaction energy H is 5.4 cm^{-1}. This appears to be in line with the type of interaction observed between the components.

[50] K. C. Gordon, J. J. McGarvey, *Inorg. Chem.* **1991**, *30*, 2986–2989.

[51] C. K. Jørgensen, *Adv. Chem. Phys.* **1963**, *5*, 33–146.

[52] a) J. W. Arbogast, C. S. Foote, M. Kao, *J. Am. Chem. Soc.* **1992**, *114*, 2277–2279; b) G. A. Heath, J. E. McGrady, R. L. Martin, *J. Chem. Soc. Chem. Commun.* **1992**, 1272–1274; c) D. M. Guldi, Hungerbühler, K.-D. Asmus, *J. Phys. Chem.* **1995**, *99*, 9380–9385.

[53] R. A. Marcus, N. Sutin, *Biochim. Biophys. Acta* **1985**, *811*, 265–322.

[54] In a classical approach, the electron-transfer rate in the nonadiabatic limit can be expressed by the following expression consisting of an electronic term (ν) and a nuclear term ($-\Delta G^{\ddagger}/RT$): $k = \nu \exp(-\Delta G^{\ddagger}/RT)$, $\nu = 2(H)^2 / h(\pi^3/\lambda RT)^{1/2}$, $\Delta G^{\ddagger} = (\lambda/4)(1 + \Delta G^0/\lambda)^2$, where λ is the reorganisation energy.[55]

[55] The reorganization energy, λ, can be described as the sum of two independent contributions, inner (bond length and angle rearrangement) and outer (solvent reorganization), with the latter being the predominant term.

$$\lambda = \lambda_o + \lambda_i$$

$$\lambda_o = e^2[(1/\varepsilon_{op}) - (1/\varepsilon_s)][(0.5\, r_D) + (0.5\, r_A) + (1/r_{DA})]$$

Replacing the pertinent parameters in the equation[53] with $r_D = 4.7$ Å, $r_A = 3.5$ Å and $r_{AD} = 14$ Å and taking $\lambda_i = 0.2$ eV, we obtain a total reorganization energy of the order of 1.2 eV.

[56] L. Isaacs, A. Wehrsig, F. Diederich, *Helv. Chim. Acta* **1993**, *76*, 1231–1250.

[57] J. N. Demas, G. A. Crosby, *J. Phys. Chem.* **1971**, *75,* 991–1024.

[58] E. M. Kober, J. V. Caspar, R. S. Lumpkin, T. J. Meyer, *J. Phys. Chem.* **1986**, *90,* 3722–3734.

[59] L. Flamigni, *J. Phys. Chem.* **1993**, *97*, 9566–9572.

[60] L. Flamigni, N. Armaroli, F. Barigelletti, V. Balzani, J.-P. Collin, J.-O. Dalbavie, V. Heitz, J.-P. Sauvage, *J. Phys Chem. B* **1997**, *101*, 5936–5943.

[61] L. Flamigni, *J. Phys. Chem.* **1992**, *96*, 3331–3373.